

Heating of the corona and acceleration of high speed solar wind

H.O. Evje¹ and E. Leer^{1,2}

¹ Institute of Theoretical Astrophysics, University of Oslo, PO Box 1029, N-0316 Oslo, Norway (h.o.evje@astro.uio.no)

² High Altitude Observatory, National Center for Atmospheric Research,* PO Box CO 3000 Boulder, USA (egil.leer@astro.uio.no)

Received 27 January 1997 / Accepted 12 September 1997

Abstract. We present a parameter study of the corona–solar wind system. The corona is heated by an energy flux from the sun. This energy flux is lost as heat conductive flux into the transition region and as solar wind energy flux. We consider two-fluid models where most of the energy flux is deposited in the proton gas. Heating of the inner corona leads to a significant (electron) heat conductive flux into the transition region and a relatively high coronal electron density. This gives a relatively low coronal proton temperature, a large solar wind proton flux, and a relatively low asymptotic flow speed. In rapidly expanding flow geometries, where the thermal coupling between electrons and protons is weaker, heating of the protons in the inner corona may lead to a somewhat higher proton temperature, and higher asymptotic flow speed, but in order to drive high speed solar wind, a significant fraction of the energy flux from the sun must be deposited in the outer corona, where the protons are collisionless. In such a model only a small fraction of the energy flux is lost as inward heat flux, the transition region pressure is low, and the solar wind proton flux is quite small. The proton temperature in the outer corona is high, and a larger fraction of the energy flux deposited in the proton gas may be lost as solar wind kinetic energy flux.

Key words: Sun: corona – solar wind – acceleration of particles

1. Introduction

The formation of the solar corona and acceleration of the solar wind was discussed by Hammer (1982a, b) and, more recently, by Hansteen & Leer (1995) and Hansteen et al. (1997). In these model studies an energy flux from the sun, deposited as heat in the extended solar atmosphere, creates a hot corona and drives the solar wind. The portion of the energy flux being conducted into the chromosphere–corona transition region and the portion lost as solar wind energy flux are determined primarily by the location of the energy deposition. Heating of the inner corona

leads to a large inward heat flux and a large transition region pressure. For extended coronal heating most of the energy flux is lost as solar wind gravitational and kinetic energy flux. Also the ratio between gravitational and kinetic energy flux in the solar wind depends upon where in the corona the energy is deposited.

In most studies of the solar wind the electrons play an important role in the force and energy balance of the flow. In thermally driven solar wind the asymptotic flow speed is generally small compared to the velocities observed in quasi-steady high speed solar wind streams in the ecliptic (e.g. Feldman et al. 1976) and at high solar latitudes, by the Ulysses spacecraft (e.g. McComas et al. 1995). In order to enhance the solar wind flow speed in these models one may allow for Alfvén waves. They propagate virtually undamped through the quasi-static corona and deposit most of their energy flux well beyond the critical point (Hollweg 1973; Leer et al. 1982), thereby increasing the asymptotic flow speed (Leer & Holzer 1980).

Low frequency Alfvén waves may propagate in the corona and in the solar wind, but they are not a likely candidate for transporting a significant energy flux into the corona from the lower solar atmosphere; the low-frequency Alfvén waves are reflected in the chromosphere–corona transition region. However, higher frequency Alfvén-mode waves, with a wavelength that is shorter than the Alfvén speed scale height, may play an important role in heating coronal holes (e.g. Parker 1991). Heating of the solar corona by relatively high frequency waves was also the physical basis for the coronal heating function used by McKenzie et al. (1995). They considered a model where all the energy flux from the sun is deposited in the proton fluid, in the inner corona. The proton heat conductive flux is taken to be zero, and all the energy flux deposited in the protons is lost as solar wind energy flux. As the solar wind mass flux is specified, the asymptotic flow speed is determined by the energy flux that is deposited in the corona. In the McKenzie et al. (1995) study the energy flux is specified such that they obtain an asymptotic flow speed that is characteristic of quasi-steady, high speed solar wind streams. But in such a model, where the proton flux is specified and all the energy flux deposited in the protons is lost in the solar wind, “any” flow speed can be obtained. However, in the Hansteen & Leer (1995) study, where proton heat conduction

* The National Center for Atmospheric Research is sponsored by the National Science Foundation

in the corona is taken into account, the asymptotic speed of the solar wind does not exceed 750 km s^{-1} .

The proton heat conductive flux in the outer corona and in the solar wind is certainly small, but in the very inner corona, where the collisional rate(s) are larger than the expansion rate, the heat flux in the proton gas and the collisional coupling to the electrons (and the electron heat conductive loss) will contribute to the transport of heat from the corona and into the transition region. This inward heat conductive flux determines the transition region pressure and the electron density in the inner corona (e.g. Withbroe 1988), and may therefore play a role in determining the solar wind mass flux.

The goal of the present study is to illustrate how heating of the coronal protons, relatively close to the sun, may produce high speed solar wind, without the deposition of an additional (e.g. Alfvén wave) energy flux in the outer solar wind. We consider two-fluid models of the corona–solar wind system. The corona is heated by a specified energy flux from the sun, and we study the structure of the corona and the solar wind proton flux and flow speed when we vary the amplitude of the energy flux from the sun, the dissipation length, and the distribution of the energy flux between electrons and protons. We make use of a “classical” expression for the proton heat conductive flux in the very inner corona, but the heat conduction coefficient is gradually reduced outwards, into the region where the protons are collisionless. We use a classical heat conductive flux for the electrons. It is shown how heating of the corona, in a region where the protons are collision-dominated, and in a region where the protons are collisionless, leads to different coronal structure and different solar wind outflow. We study both spherically symmetric flow and rapidly expanding flow geometries.

2. Equations and assumptions

We consider an electron–proton corona and assume that the gas is flowing radially without any temporal variations.

The equations for conservation of mass and momentum can be written as

$$\frac{d}{dr}(A\rho u) = 0 \quad (1)$$

and

$$\rho u \frac{du}{dr} = -\frac{dp}{dr} - \rho \frac{GM_S}{r^2} \quad (2)$$

where r is heliocentric distance, A is the cross-section of the radial flow tube, $AB = \text{constant}$, where B is the magnetic field strength, $\rho = n(m_p + m_e) = nm_p$ is the mass density, where n is the electron density and $m_{e(p)}$ is the electron (proton) mass (indices “e” and “p” are used for electrons and protons respectively), u is the flow speed, $p = p_e + p_p = nk(T_e + T_p)$ is the gas pressure, where k is Boltzmann’s constant, and $T_{e(p)}$ is the electron (proton) temperature, G is the gravitational constant, and M_S is the solar mass.

The two energy conservation equations can be written as

$$\frac{1}{A} \frac{d}{dr} \left[A \left(q_e + (1-y)f_m + \frac{5}{2}p_e u + \frac{nm_e u^2}{2} \right) \right] + \left(neE + nm_e \frac{GM_S}{r^2} \right) u - C_{ep} = 0 \quad (3)$$

and

$$\frac{1}{A} \frac{d}{dr} \left[A \left(q_p + yf_m + \frac{5}{2}p_p u + \frac{nm_p u^2}{2} \right) \right] + \left(-neE + nm_p \frac{GM_S}{r^2} \right) u - C_{pe} = 0 \quad (4)$$

where $q_{e(p)}$ is the electron (proton) heat conductive flux density, f_m is the “mechanical” energy flux density from the sun, y is the fraction of this flux that is deposited in the proton gas, and $E = -\frac{1}{en} \frac{dp_e}{dr}$ is the electric field. $C_{ep} = -C_{pe}$ is the energy transport rate per unit volume from the protons to the electrons because of Coulomb collisions, and is given by (Braginskii 1965)

$$C_{ep} = \frac{3\sigma m_e \rho^2 k(T_p - T_e)}{m_p^3 T_e^{3/2}} \quad (5)$$

where

$$\sigma = 8.36 \times 10^{-5} \text{ m}^3 \text{ K}^{3/2} \text{ s}^{-1}. \quad (6)$$

In this study we will discuss how the structure of the corona as well as the solar wind proton flux and flow speed change in models with significant coronal proton heating. The study is performed for different amplitudes and dissipation lengths of the mechanical energy flux as well as for different flow geometries. We also change the proton heat conduction and the fraction of the energy flux going into heating the electrons. The force on the plasma associated with the propagation and damping of the energy flux is neglected.

In the collision dominated quasi-static corona a classical heat flux may be used to describe the heat conduction in the proton gas. But already in the solar wind acceleration region, where the protons are close to collisionless, this may be a significant overestimate of the actual heat flux. Olsen & Leer (1996) showed that the proton heat conductive flux, found in an 8-moment fluid description, decreases rapidly in the region where the protogas becomes collisionless. This is quite close to the sun, and as an extreme case one may set $q_p = 0$ everywhere (cf. McKenzie et al. 1995). Such a model may be used to illustrate how the solar wind from a proton-heated corona is accelerated to high asymptotic flow speeds, but in more realistic models the electron–proton energy transfer and the heat conductive flux into the chromosphere–corona transition region should also be accounted for.

In a corona with comparable electron and proton heating, the electron gas is considerably colder than the proton gas due to the larger electron heat conductivity. A large fraction of the energy flux deposited in the electron fluid is conducted into the transition region, and the electron temperature will be relatively

low. The solar wind from a corona where only the electrons are heated, will have a lower speed than the wind from a corona with proton heating. In this study we therefore consider models where most of the energy flux from the sun is deposited in the proton fluid. In these models the coronal proton temperature may be large, and the asymptotic flow speed of the solar wind should also be quite large. Models with low coronal electron density should be optimal in producing a high coronal proton temperature and high speed solar wind. We allow for heating of the electrons, and to make the model as simple as possible the spatial distribution of the electron heat input is taken to be similar to the distribution of the proton heating.

In the corona and inner solar wind, where the collision time is much shorter than the expansion time, we may use a classical expression for the electron (proton) heat flux density:

$$q_{e(p)} = -\kappa_{e(p)0} T_{e(p)}^{5/2} \frac{dT_{e(p)}}{ds} \quad (7)$$

where

$$\kappa_{e0} = 7.8 \times 10^{-12} \frac{\text{J}}{\text{m s K}^{7/2}}, \quad \kappa_{p0} = 3.2 \times 10^{-13} \frac{\text{J}}{\text{m s K}^{7/2}}. \quad (8)$$

We have chosen to use this expression for q_e everywhere (cf. Lie-Svendson et al. 1997), but in the region where the proton gas is collisionless q_p must be reduced (cf. Olsen & Leer 1996). Here, we replace κ_{p0} with

$$\kappa_{p1} = \kappa_{p0} \frac{2}{1 + \exp\left(\frac{r-R_S}{h}\right)} \quad (9)$$

where h is a scale length over which the proton heat flux decreases. Notice that $\kappa_{p1} = \kappa_{p0}$ at the inner boundary, while the heat conductive flux in the proton gas is very small for $r \gg R_S + h$.

The equations for electron density, flow speed, and electron and proton temperature are solved from an inner boundary, in the upper transition region, and out to $r = 1$ AU. We specify the temperature at the inner boundary; the inner boundary is taken to be at a level in the upper transition region where we ensure that the electrons and protons are thermally coupled. In the present study the inner boundary is at a level where the temperature is $T_0 = 700\,000$ K.

In self consistent models of hydrogen outflow from the chromosphere, through the transition region and corona, and into interplanetary space, it is found that the transition region pressure (and the electron density in the inner corona) is determined by the heating of the transition layer and the heat conductive flux from the corona (Hansteen & Leer 1995). When there is no energy deposition in the transition region, and the solar wind enthalpy flux at the inner boundary is small compared to the radiative loss from the transition region, the pressure is, to a good approximation, proportional to the inward heat conduction flux density, $-q_0$ (Landini & Monsignori-Fossi 1973):

$$2n_0 k T_0 \approx C(-q_0) \quad (10)$$

where C is a constant.

This approximation may be used in spherically symmetric flow, but in a rapidly expanding flow, where the solar wind is originating from a small area, the solar wind enthalpy flux at the inner boundary (where $T_0 = 700\,000$ K) is larger than the radiative loss from the transition region. At the inner boundary we therefore have that

$$-q_0 \approx 2n_0 k T_0 / C + 5k T_0 (nu)_0, \quad (11)$$

i.e. the inward heat flux balances the radiative loss and the increase of the solar wind enthalpy flux in the transition region. Then the electron density at the inner boundary is given by

$$n_0 = \frac{-q_0}{k T_0 \left(5u_0 + \frac{2}{C}\right)}. \quad (12)$$

This is the boundary condition used in the present study. The constant C is set to

$$C = 7.5 \times 10^{-5} \text{ s m}^{-1}. \quad (13)$$

Any mechanical heating of the transition region would be equivalent to a larger inward heat conduction, and therefore increased left side of Eq. (11). This leads to higher density, n_0 , or proton flux density, $(nu)_0$, or both.

In most of this study we will consider self consistent models, where the electron density, n_0 , at the inner boundary, is determined by Eq. (12). In contrast, in many model studies of the corona–solar wind system the density at the inner boundary is specified, independently of the inward heat flux. We will also consider such models.

3. Results

3.1. Spherically symmetric flow

Let us first consider spherically symmetric flow, i.e. $A \propto r^2$. The electron density at the inner boundary, $r_0 = 1.0 R_S$, where $T_0 = 700\,000$ K, satisfies Eq. (12). This means that the radiative losses at and above the top of the chromosphere, as well as the increase of the solar wind enthalpy flux through the transition region, are balanced by the inward heat flux. This procedure allows us to treat the formation of the corona and acceleration of the solar wind in a self consistent manner.

We want to study models where the corona is heated relatively close to the sun. We specify the mechanical energy flux density from the sun, f_{m0} , at the inner boundary. The mechanical energy flux, F_m , in the $A \propto r^2$ flow tube is transferred to the corona as heat over a damping length H_m :

$$F_m = A f_m = A_0 f_{m0} \exp\left(-\frac{r - R_S}{H_m}\right). \quad (14)$$

This simple model of the coronal heating may not be realistic, but model studies with different damping lengths, H_m , and different energy flux densities, f_{m0} , should help us understand how the location and amplitude of the coronal heating determine the structure of the corona and the solar wind proton flux and asymptotic flow speed. We choose a set of parameter values, $f_{m0} = 100 \text{ W m}^{-2}$, $H_m = 1.0 R_S$, $y = 90\%$, and $h = 0.3 R_S$, and vary them, one at a time, to see the effect of each parameter.

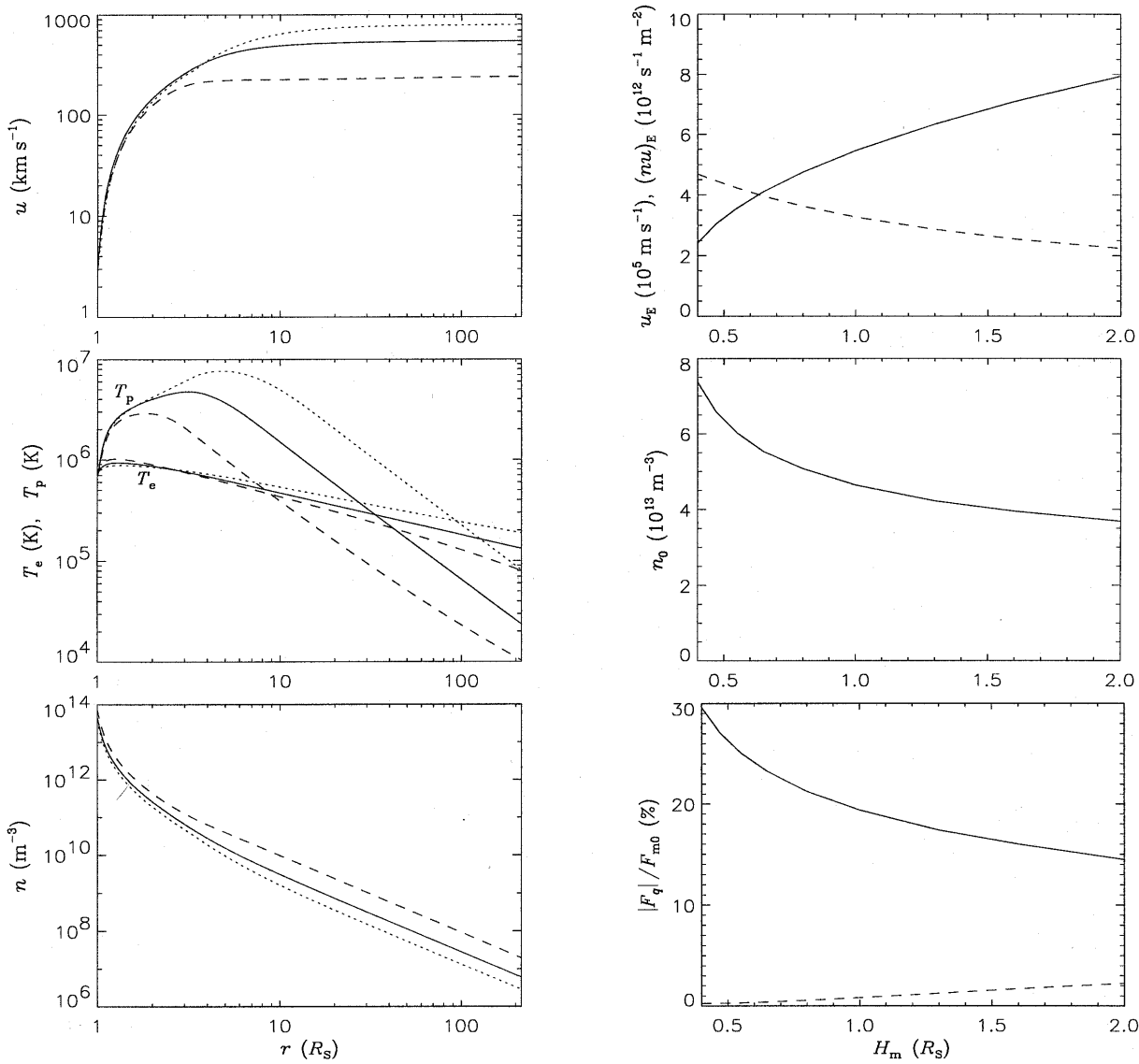


Fig. 1. Results from the model with $A \propto r^2$ geometry. The proton heat conduction parameter is $h = 0.3 R_S$. The input mechanical energy flux density is $f_{m0} = 100 \text{ W m}^{-2}$, the protons get $y = 90\%$ of this energy flux, and the damping length, H_m , is varied. In the left column the flow speed, u , electron and proton temperatures, T_e and T_p , and electron density, n , are plotted versus heliocentric distance, r , for $H_m = 0.4 R_S$ (dashed line), $H_m = 1.0 R_S$ (solid line) and $H_m = 2.0 R_S$ (dotted line). In the right column the top panel shows the flow speed, u_E , (solid line) and proton flux density, $(\nu u)_E$, (dashed line) at $r = 1 \text{ AU}$, the middle panel shows the electron density, n_0 , at the inner boundary, $r = r_0 = R_S$, and the bottom panel shows the fraction of the energy flux from the sun that is lost as heat conductive flux into the inner boundary (solid line) and as heat conductive flux at $r = 1 \text{ AU}$ (dashed line), versus H_m .

3.1.1. Variation of the damping length, H_m

We choose the base values for all the parameters, but vary the damping length: The mechanical energy flux density from the sun is $f_{m0} = 100 \text{ W m}^{-2}$, the protons get $y = 90\%$ of this energy flux while the electrons get the remaining 10% , and the proton heat conduction coefficient is given by Eq. (9) with $h = 0.3 R_S$. The damping length, H_m , is varied from $0.4 R_S$ to $2.0 R_S$. The results are plotted in Fig. 1.

The left column of Fig. 1 shows the flow speed, u , the electron and proton temperature, T_e and T_p , and the electron density, n , as a function of heliocentric distance, r , for $H_m = 0.4 R_S$,

$1.0 R_S$, and $2.0 R_S$. For the base values of the model parameters, i.e. for $H_m = 1.0 R_S$, we find that the proton temperature reaches a maximum of $4.8 \times 10^6 \text{ K}$ at $r = 3.1 R_S$. The electron temperature maximum is only $9.3 \times 10^5 \text{ K}$. The solar wind has an asymptotic flow speed of about 550 km s^{-1} , and the solar wind proton flux density is $3.3 \times 10^{12} \text{ m}^{-2} \text{ s}^{-1}$ at $r = 1 \text{ AU}$. The proton gas is assumed to be adiabatic in the outer solar wind, so the proton temperature is low, $T_{pE} = 2.4 \times 10^4 \text{ K}$, at the orbit of Earth. The electron temperature at $r = 1 \text{ AU}$ is $T_{eE} = 1.3 \times 10^5 \text{ K}$.

We see that the proton temperature maximum increases with increasing damping length, from 2.9×10^6 K for $H_m = 0.4 R_S$ to 7.7×10^6 K for $H_m = 2.0 R_S$, whereas the coronal electron temperature does not vary significantly when the damping length increases. A high coronal proton temperature is consistent with a high asymptotic flow speed, and we find that it is about 800 km s^{-1} for $H_m = 2.0 R_S$.

The density decrease, with heliocentric distance, in the inner corona is like the density fall-off in a static corona, and the density profile gradually approaches an $n \propto r^{-2}$ -profile in the outer solar wind. The differences in the electron density profiles, displayed in the lower left panel, are caused by an increase of the asymptotic flow speed and a decrease of the solar wind proton flux with increasing damping length, H_m .

The right column of Fig. 1 shows how some quantities vary with the damping length, H_m . The upper right panel shows that the proton flux density at $r = 1 \text{ AU}$ decreases from $(nu)_E = 4.7 \times 10^{12} \text{ s}^{-1} \text{ m}^{-2}$ for $H_m = 0.4 R_S$ to $(nu)_E = 2.2 \times 10^{12} \text{ s}^{-1} \text{ m}^{-2}$ for $H_m = 2.0 R_S$. The flow speed at the orbit of Earth increases from $u_E = 240 \text{ km s}^{-1}$ for $H_m = 0.4 R_S$ to $u_E = 790 \text{ km s}^{-1}$ for $H_m = 2.0 R_S$. The decreasing proton flux is consistent with an increase of the asymptotic flow speed because most of the energy flux deposited in the extended corona is lost as solar wind energy flux.

When the inner corona is heated, as it is when $H_m = 0.4 R_S$, the protons loose energy through inward heat conduction and to the electrons because of strong collisional coupling in the inner region. The lower right panel in Fig. 1 shows that in this case almost 30% of the energy flux deposited in the corona is transported back to the sun as heat conductive flux. The outward heat conduction at $r = 1 \text{ AU}$ is negligible. One-third of the inward heat flux goes into heating of the solar wind in the transition region, while two-third is radiated away. This determines the density at the inner boundary, n_0 , shown in the middle panel in the right column, and for $H_m = 0.4 R_S$ it is $n_0 = 7.4 \times 10^{13} \text{ m}^{-3}$. For an increasing damping length the inward heat conduction decreases rapidly. Since most of the inward heat conductive flux is lost as radiation, n_0 is approximately proportional to the inward heat flux. When $H_m = 2.0 R_S$ the inward heat conductive flux is only 14% of the input mechanical energy flux, and $n_0 = 3.7 \times 10^{13} \text{ m}^{-3}$.

3.1.2. Variation of the energy input, f_{m0}

We have now studied how variations of the damping length, H_m , affect the structure of the corona and the solar wind proton flux and flow speed. Let us see what influence the amplitude of the mechanical energy flux density, f_{m0} , has on the results. The other model parameters are set to their base values: $H_m = 1.0 R_S$, $h = 0.3 R_S$ and $y = 90\%$. The results are presented in Fig. 2.

The left column in Fig. 2 shows the flow speed, u , (upper panel), and the electron and proton temperature, T_e and T_p , (lower panel) versus heliocentric distance, r , for $f_{m0} = 50 \text{ W m}^{-2}$, $f_{m0} = 100 \text{ W m}^{-2}$, and $f_{m0} = 200 \text{ W m}^{-2}$. We see only small variations in these quantities when the energy flux from the sun changes.

The upper right panel in Fig. 2 shows that the solar wind proton flux density at $r = 1 \text{ AU}$, $(nu)_E$, increases linearly from $1.6 \times 10^{12} \text{ s}^{-1} \text{ m}^{-2}$ to $6.3 \times 10^{12} \text{ s}^{-1} \text{ m}^{-2}$ when f_{m0} changes from 50 W m^{-2} to 200 W m^{-2} , and that the flow speed at $r = 1 \text{ AU}$, u_E , increase from 510 km s^{-1} to 600 km s^{-1} in the same range of f_{m0} -values. The lower right panel shows that the electron density at the inner boundary, n_0 , also increases with f_{m0} , but the inward heat conductive flux increases somewhat slower than linearly with f_{m0} , and this trend is reflected in the increase of n_0 . For the increase of f_{m0} from 50 W m^{-2} to 200 W m^{-2} n_0 increases from $3.3 \times 10^{13} \text{ m}^{-3}$ to $6.4 \times 10^{13} \text{ m}^{-3}$. Fig. 2 shows that the solar wind proton flux is proportional to the energy flux density, f_{m0} , whereas the variations in the temperature profiles and in the solar wind flow speed are relatively small.

3.1.3. Variation of the proton heat conduction, h

We know that the classical proton heat conductive flux is an overestimate of the proton heat flux in the outer corona and in the solar wind. In our model we allow for classical heat conduction in the inner corona, and make use of the parameter h to reduce the heat conduction coefficient with increasing heliocentric distance. Let us now study the effect of ‘‘cutting off’’ the heat conduction in the proton gas, at different heliocentric distances, by varying this parameter from $h = 0.1$ to $2.0 R_S$, i.e. we go from a model with classical proton heat conduction only in the very inner corona to a model with classical heat conduction out to several solar radii. The other parameters are set to their base values: $f_{m0} = 100 \text{ W m}^{-2}$, $H_m = 1.0 R_S$, and $y = 90\%$. The results are shown in Fig. 3.

The left column shows the flow speed, u , (upper panel) and the electron and proton temperature, T_e and T_p , (lower panel) along the radial flow tube for $h = 0.1 R_S$, $h = 0.3 R_S$ and $h = 2.0 R_S$. We see that the temperature profiles are similar *in the very inner corona*, but for the case with $h = 2 R_S$ the proton temperature reaches a maximum of $3.3 \times 10^6 \text{ K}$, whereas in the $h = 0.1 R_S$ case the proton temperature reaches $8.2 \times 10^6 \text{ K}$. In this case a significant fraction of the energy flux is deposited in the region where there is almost no proton heat conductive flux, so the heat flux from the corona and into the inner boundary, is reduced. Hence, the electron density at the inner boundary is reduced, and the solar wind proton flux is reduced. As the energy flux from the sun is fixed, $f_{m0} = 100 \text{ W m}^{-2}$, the asymptotic flow speed is increased, from 490 km s^{-1} for $h = 2 R_S$ to 750 km s^{-1} for $h = 0.1 R_S$ (see upper left panel). Notice that the increase of h from $0.1 R_S$ to $0.3 R_S$ is enough to reduce the asymptotic flow speed from 750 km s^{-1} to 550 km s^{-1} . A further increase of h has a relatively small effect on the asymptotic flow speed. The electron temperature profile is almost the same in all cases.

The right column shows the flow speed, u_E , and the proton flux density, $(nu)_E$, at $r = 1 \text{ AU}$ (upper panel) and the electron density, n_0 , at the inner boundary (lower panel). Again we see that there are significant changes for small values of h . With classical proton heat conduction only in the inner corona, and

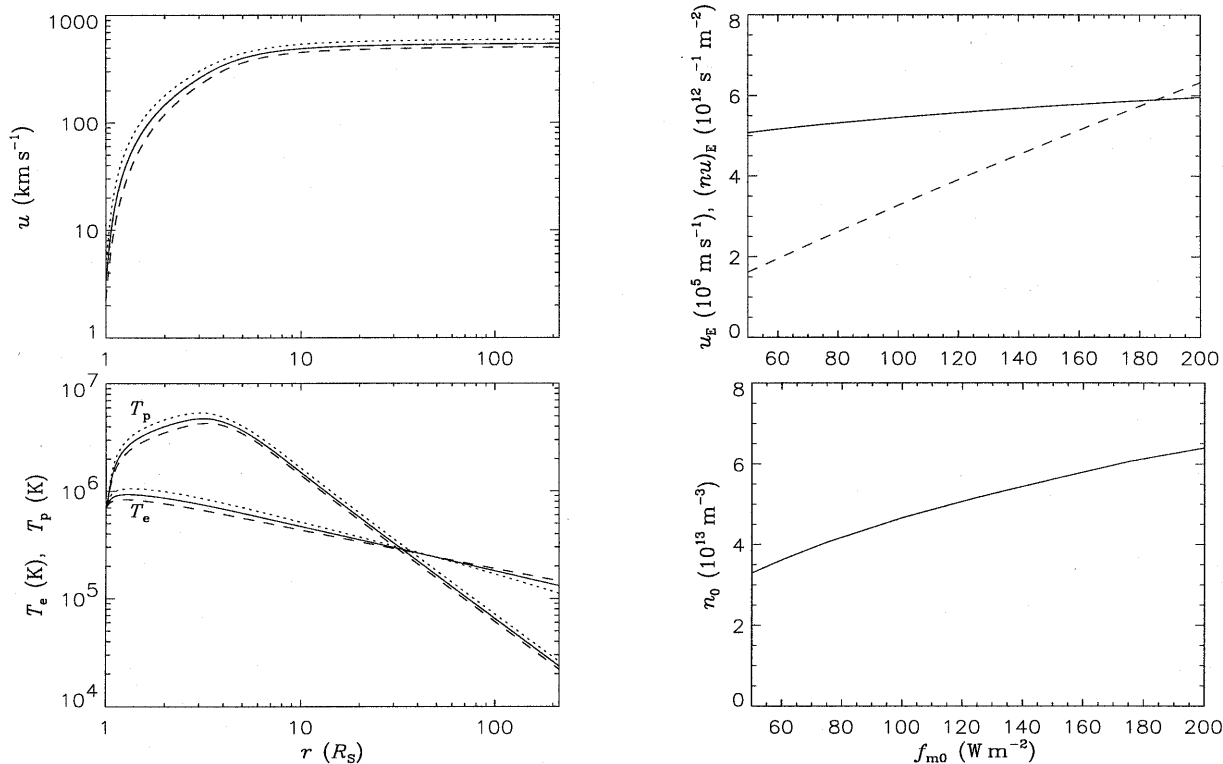


Fig. 2. Results from the model with $A \propto r^2$ geometry. The proton heat conduction parameter is $h = 0.3 R_S$. The mechanical energy flux' damping length is $H_m = 1.0 R_S$, $y = 90\%$ of the energy flux goes into the protons, and the input mechanical energy flux density, f_{m0} , is varied. In the left column the flow speed, u , and the electron and proton temperatures, T_e and T_p , are plotted versus heliocentric distance, r , for $f_{m0} = 50 \text{ W m}^{-2}$ (dashed line), $f_{m0} = 100 \text{ W m}^{-2}$ (solid line) and $f_{m0} = 200 \text{ W m}^{-2}$ (dotted line). In the right column the top panel shows the flow speed, u_E , (solid line) and proton flux density, $(nu u)_E$, (dashed line) at $r = 1 \text{ AU}$, and the bottom panel shows the electron density, n_0 , at the inner boundary, $r = r_0 = R_S$, versus f_{m0} .

no proton heat flux in the outer corona, i.e. h small, the heat conductive flux into the transition region is small, and the electron density, n_0 , and the proton flux, $(nu u)_E$, are low, while the asymptotic flow speed is high. For h increasing from 0.1 to $2.0 R_S$, u_E decreases from 750 km s^{-1} to 490 km s^{-1} while $(nu u)_E$ increases from $2.4 \times 10^{12} \text{ s}^{-1} \text{ m}^{-2}$ to $3.5 \times 10^{12} \text{ s}^{-1} \text{ m}^{-2}$ and n_0 increases from $3.5 \times 10^{13} \text{ m}^{-3}$ to $5.3 \times 10^{13} \text{ m}^{-3}$.

3.1.4. Variation of the proton heating, y

Now we will vary the energy distribution between protons and electrons, which is determined by the parameter y . The other parameters are set to their base values: $f_{m0} = 100 \text{ W m}^{-2}$, $H_m = 1.0 R_S$ and $h = 0.3 R_S$. The results are shown in Fig. 4.

The left column shows the flow speed, u , (upper panel) and the electron and proton temperatures, T_e and T_p , versus heliocentric distance, r , for $y = 50\%$, $y = 90\%$ and $y = 100\%$. The figure shows that an increase of y leads to an increase of the maximum proton temperature and the asymptotic flow speed, and a decrease of the maximum electron temperature, but the flow speed profiles and temperature profiles in the corona, obtained for $y = 90\%$ and $y = 100\%$, are not very different. With $y = 100\%$ the only heating of the electrons is by collisions with

protons. In this case the electrons become almost adiabatic at $r = 1 \text{ AU}$.

In the upper panel of the right column we show the solar wind flow speed, u_E , and the proton flux density, $(nu u)_E$, at the orbit of Earth, versus y , and in the lower panel the electron density, n_0 , at the inner boundary is plotted, also as a function of y . We see that both the flow speed and the proton flux density at $r = 1 \text{ AU}$ increase when y increase from 50% to 100%. This is possible because the inward heat conductive flux from the corona decreases when y increases, and more of the energy flux is available for driving the solar wind. For the parameters used here the flow speed and proton flux do not change dramatically, even for the relatively large variations in y . If we had varied y in a model with a smaller h -value and a larger value of H_m , we would have found a larger variation in the flow speed and the proton flux than in the model considered.

The lower panel of the right column shows the electron density, n_0 , at the inner boundary as a function of y . As the electrons easily conduct heat into the transition region, n_0 is largest when a large fraction of the mechanical energy flux from the sun is deposited in the electron fluid. For $y = 50\%$ we have that $n_0 = 7.3 \times 10^{13} \text{ m}^{-3}$, whereas for $y = 100\%$ we find that n_0 is reduced to $4.4 \times 10^{13} \text{ m}^{-3}$. But the high density for $y = 50\%$

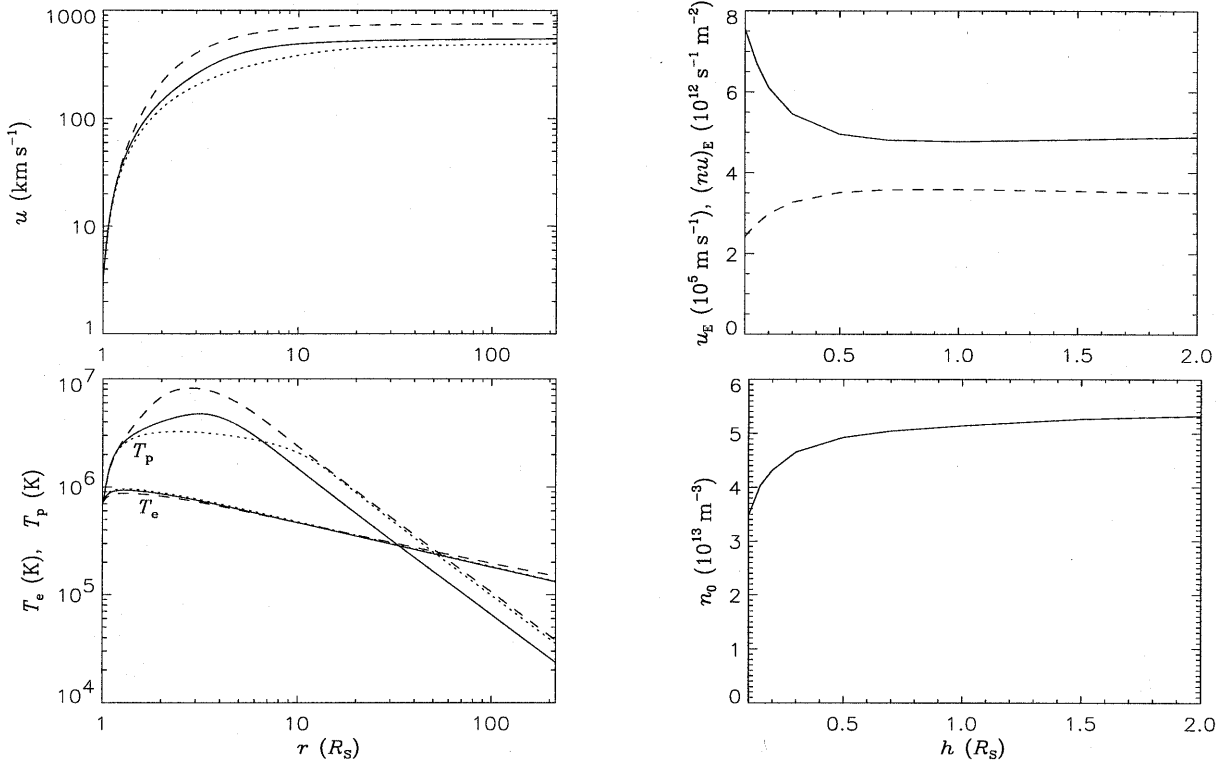


Fig. 3. Results from the model with $A \propto r^2$ geometry. The input mechanical energy flux density is $f_{m0} = 100 \text{ W m}^{-2}$, the protons get $y = 90\%$ of this energy flux, and the damping length is $H_m = 1.0 R_S$. The proton heat conduction parameter, h , is varied. In the left column the flow speed, u , and the electron and proton temperatures, T_e and T_p , are plotted versus heliocentric distance, r , for $h = 0.1 R_S$ (dashed line), $h = 0.3 R_S$ (solid line) and $h = 2.0 R_S$ (dotted line). In the right column the top panel shows the flow speed, u_E , (solid line) and proton flux density, $(\nu u)_E$, (dashed line) at $r = 1 \text{ AU}$, and the bottom panel shows the electron density, n_0 , at the inner boundary, $r = r_0 = R_S$, versus h .

does not correspond to a large solar wind proton flux. The lower mean temperature in the inner corona makes the density scale height short, and the higher temperature in the $y = 100\%$ case leads to a higher proton flux, in spite of the lower value of n_0 .

3.2. Rapidly expanding flow geometry

The results obtained for an $A \propto r^2$ geometry show that a small damping length, say $H_m \approx 0.5 R_S$, does not produce high speed solar wind. This result does not seem to be in agreement with the results found by McKenzie et al. (1995). They considered a two-fluid solar wind model, with proton heating and with no heat conduction in the proton gas, and they used a rapidly expanding flow geometry. Let us now study a model with their geometry and their coronal heating function.

The expansion of their radial flow tube is given by $A \propto B^{-1}$ where

$$B(r) \propto \frac{2}{r^3} + \frac{1}{a(a+r)^2} \quad (15)$$

and $a \approx 3.98 R_S$, and their heating function is

$$Q = -\frac{1}{A} \frac{dF_m}{dr} = Q_0 \exp\left(-\frac{r-R_S}{L}\right). \quad (16)$$

In this model the expansion of the flow tube is approximately a factor 8 larger than the expansion of an $A \propto r^2$ flow tube. It should be pointed out that the characteristic length of variation, L , for the heating function is considerably shorter than a characteristic length of variation for the corresponding energy flux,

$$F_m = -\int_{\infty}^r A Q_0 \exp\left(-\frac{r-R_S}{L}\right) dr. \quad (17)$$

With the coronal heating function in Eq. (16), the mechanical energy flux, F_m , in the flow tube is damped more slowly in the inner corona, and more rapidly in the outer corona than an energy flux with a constant damping length, H_m . For $L = 0.20, 0.30$ and $0.50 R_S$ the energy flux from the sun, F_{m0} , is reduced by a factor e over a distance $H = 0.34, 0.62$ and $1.29 R_S$ respectively.

Notice that the energy flux density at the inner boundary in this model is

$$f_{m0} = -\frac{1}{A_0} \int_{\infty}^{R_S} A Q dr. \quad (18)$$

3.2.1. Variation of the damping length, L

Also in this model the inner boundary is taken at a level where the temperature is $T_0 = 700\,000 \text{ K}$, and the electron density, n_0 , at

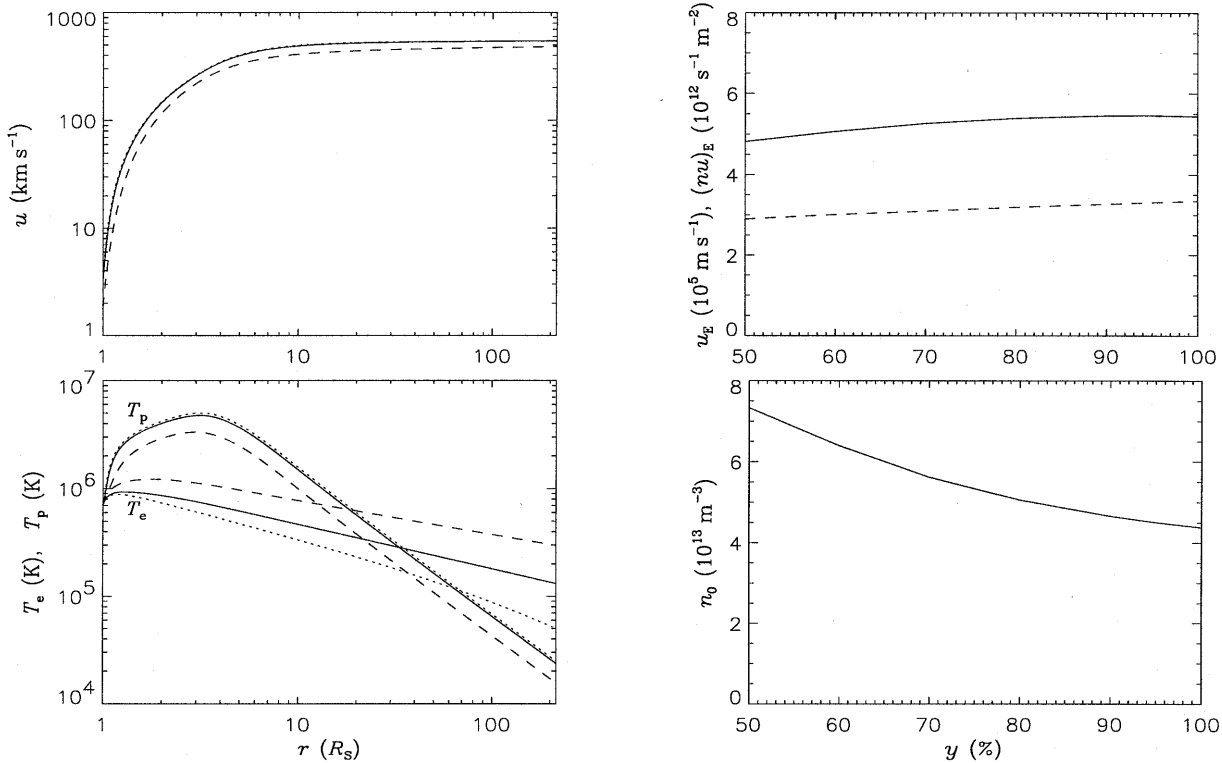


Fig. 4. Results from the model with $A \propto r^2$ geometry. The mechanical energy flux density at the inner boundary is $f_{m0} = 100 \text{ W m}^{-2}$. The mechanical energy flux' damping length is $H_m = 1.0 R_S$, the proton heat conduction parameter $h = 0.3 R_S$, and the part of the energy flux absorbed by the protons, y , is varied. In the left column the flow speed, u , and the electron and proton temperatures, T_e and T_p , are plotted versus heliocentric distance, r , for $y = 50\%$ (dashed line), $y = 90\%$ (solid line) and $y = 100\%$ (dotted line). In the right column the top panel shows the flow speed, u_E , (solid line) and proton flux density, $(nu u)_E$, (dashed line) at $r = 1 \text{ AU}$, and the bottom panel shows the electron density, n_0 , at the inner boundary, $r = r_0 = R_S$, versus y .

the inner boundary is given by Eq. (12). The collisional coupling is strong at the inner boundary. In the rapidly expanding flow, considered here, the cross-section of the flow tube increases with a factor 8 compared to the cross-section of a flow tube in an $A \propto r^2$ flow geometry, so we increase the base value of the energy flux density at the inner boundary to $f_{m0} = 800 \text{ W m}^{-2}$. The base values for the other model parameters are $L = 0.3 R_S$, $y = 90\%$, and $h = 0.3 R_S$. Let us first vary the damping length L . The results are presented in Fig. 5.

The left column of Fig. 5 shows flow speed, u , (upper panel) and electron and proton temperature, T_e and T_p , (lower panel) versus heliocentric distance, r , for $L = 0.20 R_S$, $L = 0.30 R_S$, and $L = 0.50 R_S$. For the base value, $L = 0.3 R_S$, the coronal proton temperature reaches a maximum of $5.7 \times 10^6 \text{ K}$. This is sufficient to accelerate the flow to an asymptotic flow speed of 610 km s^{-1} . For the smaller L -value, $L = 0.20 R_S$, the proton temperature is reduced and the solar wind reaches a lower speed, $u_E = 440 \text{ km s}^{-1}$. For $L = 0.50 R_S$ we find a maximum proton temperature of $8.5 \times 10^6 \text{ K}$ and an asymptotic flow speed of 850 km s^{-1} . The electron temperature in the outer solar wind changes when L is varied, but the changes of the coronal electron temperature are small. We see that even for the smallest L value the proton temperature reaches almost $5 \times 10^6 \text{ K}$, and the solar

wind is accelerated to more than 400 km s^{-1} at the orbit of Earth. So heating close to the sun produces a higher flow speed in a rapidly expanding flow geometry than in spherically symmetric outflow.

In the upper right panel we show the flow speed, u_E , and proton flux, $(nu u)_E$, at $r = 1 \text{ AU}$, versus the characteristic length, L , and in the lower right panel we show the variation of the coronal base electron density, n_0 . The tendencies are the same as when we varied H_m in the spherically symmetric flow (cf. Fig. 1): Extended coronal heating leads to higher asymptotic flow speed, lower proton flux, and lower electron density at the inner boundary. More specifically $L = 0.20 R_S$ gives $u_E = 440 \text{ km s}^{-1}$, $(nu u)_E = 4.4 \times 10^{12} \text{ s}^{-1} \text{ m}^{-2}$ and $n_0 = 9.1 \times 10^{13} \text{ m}^{-3}$, whereas $L = 0.50 R_S$ gives $u_E = 850 \text{ km s}^{-1}$, $(nu u)_E = 2.3 \times 10^{12} \text{ s}^{-1} \text{ m}^{-2}$ and $n_0 = 5.4 \times 10^{13} \text{ m}^{-3}$.

For $L = 0.4 - 0.5 R_S$ we obtain asymptotic flow speeds that are in fairly good agreement with observations of quasi-steady high speed solar wind (McComas et al. 1995; Phillips et al. 1995), and the high coronal proton temperatures, consistent with these high flow speeds, are in good agreement with the proton temperatures derived from the $Ly - \alpha$ observations in large coronal holes (Kohl et al. 1996). Notice that the large flow speeds are obtained when a significant fraction of the energy

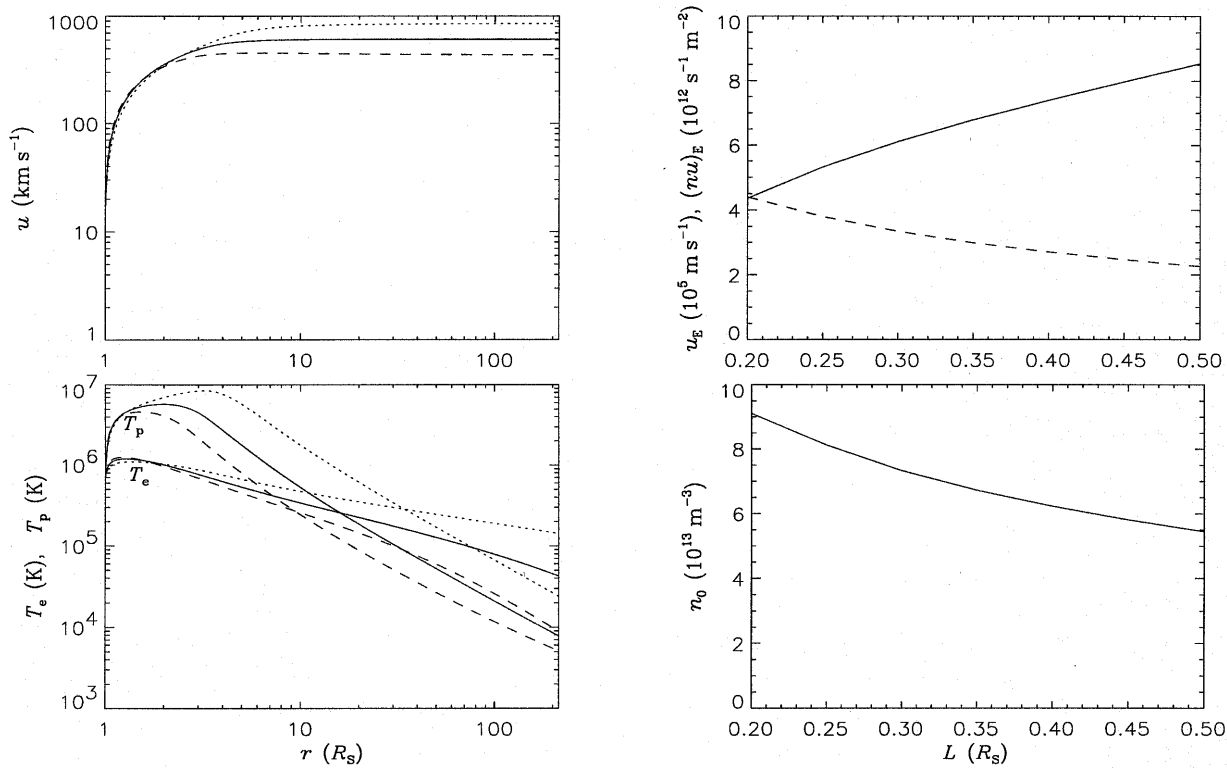


Fig. 5. Results from the model with rapidly expanding geometry when the characteristic length, L , of the heating function, Q , is varied. The input mechanical energy flux density is $f_{m0} = 800 \text{ W m}^{-2}$, and $y = 90\%$ of this energy flux is absorbed by the protons. The proton heat conduction parameter is $h = 0.3 R_S$. In the left column the radial profiles of the flow speed, u , and the electron and proton temperature, T_e and T_p , are shown for $L = 0.2 R_S$ (dashed line), $L = 0.3 R_S$ (solid line) and $L = 0.5 R_S$ (dotted line). In the right column the top panel shows the speed at the orbit of Earth, u_E , (solid line) and proton flux density, $(\nu u)_E$, (dashed line), and the bottom panel shows the electron density, n_0 , at the inner boundary, at $r = r_0 = R_S$, versus L .

flux from the sun is deposited in the region where the proton heat conductive flux is small. Let us also illustrate the effect of shifting the proton heating from the collision dominated region and into the collisionless region by holding L constant and varying the parameter h .

3.2.2. Variation of the proton heat conduction, h

The parameter h determines how far into the corona the classical expression can be used to describe the proton heat flux. For $r \gg R_S + h$ the proton heat flux is negligible. Let us now vary h . The other parameters have their base values: $f_{m0} = 800 \text{ W m}^{-2}$, $L = 0.3 R_S$, and $y = 90\%$. The results are shown in Fig. 6.

The left column shows the flow speed, u , (upper panel) and proton and electron temperature, T_p and T_e , versus heliocentric distance, r , from the inner boundary and out to the orbit of Earth. We show results for $h = 0.1, 0.3$, and $2.0 R_S$. For the base value, $h = 0.3 R_S$, we find an asymptotic flow speed of 610 km s^{-1} and a proton temperature maximum, at $r \approx 2.0 R_S$, of $5.7 \times 10^6 \text{ K}$. A reduction of the region where proton heat conduction is important, by reducing h from $0.3 R_S$ to $0.1 R_S$, leads to an enhanced coronal proton temperature, with a maximum of $8.2 \times 10^6 \text{ K}$, and an enhanced asymptotic flow speed of 740 km s^{-1} . An extension of the region where heat conduction in the proton

gas is important, by increasing h to $2.0 R_S$, leads to a somewhat lower and broader proton temperature maximum in the corona, but the asymptotic flow speed is virtually unchanged.

In the right panel we show variations of some solar wind and corona parameters, as a function of h . The flow speed, u_E , and the proton flux density, $(\nu u)_E$, at $r = 1 \text{ AU}$ are shown in the upper right panel. In the lower right panel we show the electron density, n_0 , at the inner boundary. The asymptotic flow speed decreases and the solar wind proton flux increases with increasing values of h , but for $h > 0.3 R_S$ the variations are relatively small. The heat conductive flux into the transition region is small in the case of small h -values, and the solar wind proton flux is small. However, in this rapidly expanding flow the electron density at the inner boundary is almost constant when h is varied from $0.1 R_S$ to $2.0 R_S$ (lower right panel). Most of the heat flux into the transition region goes into heating the flow. Thus, the solar wind proton flux increases with increasing h -values, but n_0 is almost unchanged.

These results show that we obtain more or less the same solar wind proton flux and asymptotic flow speed when the coronal protons are heated in a region where classical proton heat conduction can distribute the heat within the proton gas. When most of the heating takes place in a region where there is almost

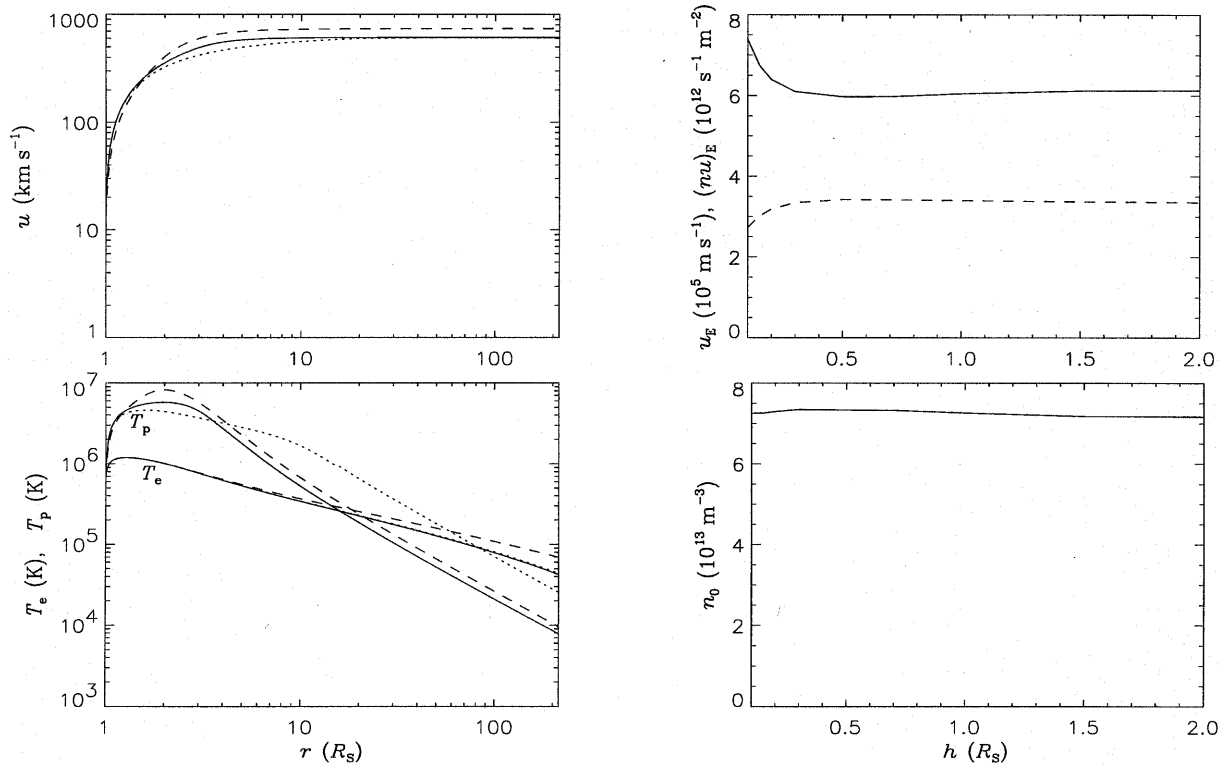


Fig. 6. Results from the model with rapidly expanding geometry. The mechanical energy flux density at the inner boundary is $f_{m0} = 800 \text{ W m}^{-2}$. The characteristic length, L , of the heating function, Q , is $L = 0.30 R_S$, $y = 90\%$ of the energy flux goes into the protons, and the proton heat conduction parameter h is varied. In the left column the flow speed, u , and the electron and proton temperatures, T_e and T_p , are plotted versus heliocentric distance, r , for $h = 0.1 R_S$ (dashed line), $h = 0.3 R_S$ (solid line) and $h = 2.0 R_S$ (dotted line). In the right column the top panel shows the flow speed, u_E , (solid line) and proton flux density, $(\nu u)_E$, at $r = 1 \text{ AU}$, and the bottom panel shows the electron density, n_0 , at the inner boundary, $r = r_0 = R_S$, versus h .

no proton heat conduction, and the coupling to the electrons is weak, the solar wind proton flux is reduced, the maximum coronal proton temperature is increased, and the asymptotic flow speed of the solar wind is also increased.

3.3. Constant density at the inner boundary

In most model studies of the solar wind the electron density is specified at an inner boundary, the coronal base, and it is not adjusted to the inward heat flux. Let us now consider such models to see how sensitive the solar wind flow speed and proton flux are to variations in the electron density at the inner boundary.

To make this as simple as possible, we set the proton heat flux equal to zero, $q_p = 0$, everywhere in the model. This assumption leads to higher proton temperatures and higher flow speeds than what we would get if a reasonable proton heat flux were included. The inner boundary is, as in our previous models, placed at $r_0 = 1.0 R_S$, where $T_0 = 700\,000 \text{ K}$, and we let the protons get $y = 90\%$ of the energy flux from the sun. We consider both spherically symmetric flow, $A \propto r^2$, where the energy flux density at the inner boundary is $f_{m0} = 100 \text{ W m}^{-2}$, and the rapidly expanding flow geometry with $f_{m0} = 800 \text{ W m}^{-2}$. The electron densities at the inner boundary is in the range $2 \times 10^{13} \text{ m}^{-3}$ to $2 \times 10^{14} \text{ m}^{-3}$.

The left column in Fig. 7 shows results for the $A \propto r^2$ -model, the right column is for the rapidly expanding flow. The variation of flow speed, u_E , (upper panels) and proton flux density, $(\nu u)_E$, (lower panels) at $r = 1 \text{ AU}$ with increasing damping length, H_m or L , are plotted for three values of the coronal base electron density, $n_0 = 2.0 \times 10^{13} \text{ m}^{-3}$, $6.0 \times 10^{13} \text{ m}^{-3}$, and $2.0 \times 10^{14} \text{ m}^{-3}$. The results are qualitatively similar in these two models: For a given electron density in the inner corona, the asymptotic flow speed increases and the proton flux decreases with increasing values of H_m or L . This is the same result as we found in the self-consistent models, where the electron density at the inner boundary was adjusted to the heat flux into the transition region (cf. Fig. 1 and Fig. 5); For a lower coronal base electron density the asymptotic flow speed is higher, and the solar wind proton flux is lower. The main difference between the two geometries is that in rapidly expanding flow one can obtain very large asymptotic flow speeds even for small damping lengths. For a coronal base density of $n_0 = 2.0 \times 10^{13} \text{ m}^{-3}$ we find $u_E = 1120 \text{ km s}^{-1}$ for $L = 0.2 R_S$. ($L = 0.20 R_S$ corresponds to a damping length for the energy flux of $H_m \approx 0.34 R_S$.) For the same coronal base electron density and $H_m = 0.40 R_S$ we find $u_E = 570 \text{ km s}^{-1}$ in the $A \propto r^2$ -model.

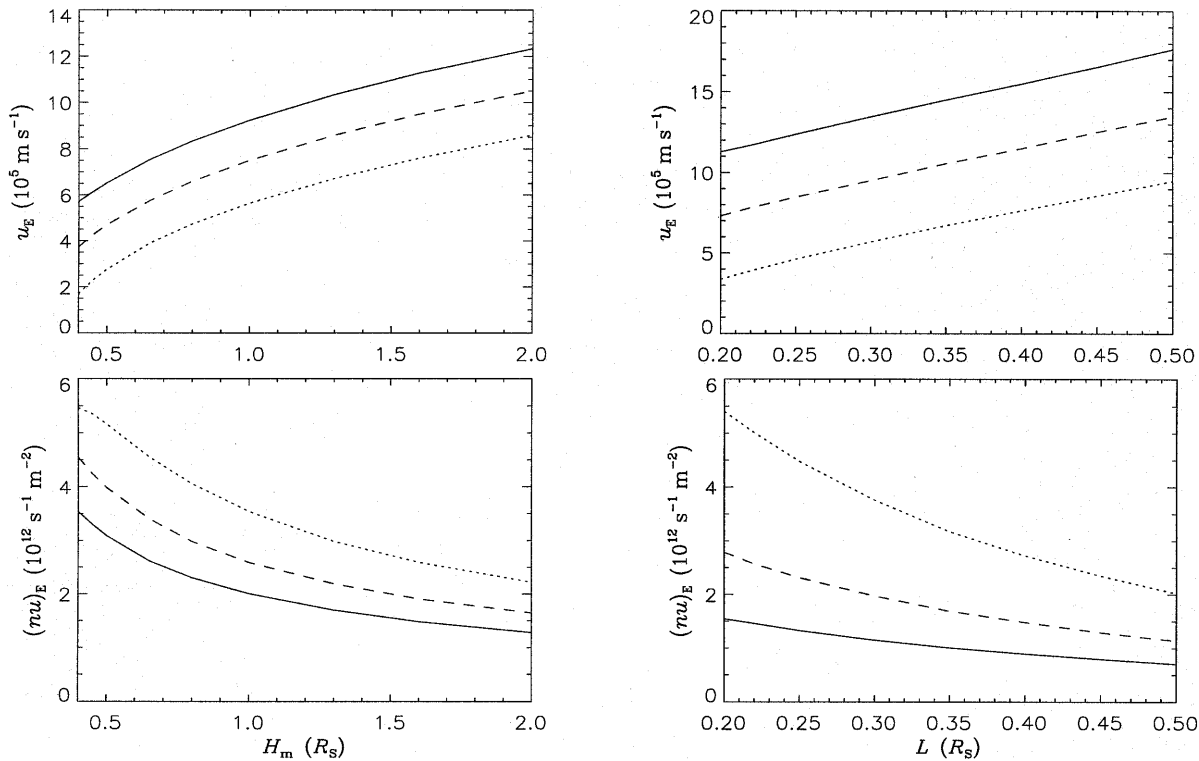


Fig. 7. Results from models where the electron density, n_0 , at the inner boundary, $r = r_0 = R_S$, is specified; it is *not* determined by the inward heat conductive flux. There is no proton heat conduction, and the protons get $\gamma = 90\%$ of the energy flux. The left column shows results from the model with $A \propto r^2$ geometry and a mechanical energy flux from the sun of $f_{m0} = 100 \text{ W m}^{-2}$. The right column shows results from the model with a more rapidly expanding geometry and $f_{m0} = 800 \text{ W m}^{-2}$. The flow speed, u_E , (top panels) and proton flux density, $(nu)_E$, (bottom panels) at $r = 1 \text{ AU}$ are plotted as functions of H_m and L for $n_0 = 2.0 \times 10^{13} \text{ m}^{-3}$ (solid line), $n_0 = 6.0 \times 10^{13} \text{ m}^{-3}$ (dashed line), and $n_0 = 2.0 \times 10^{14} \text{ m}^{-3}$ (dotted line).

On the other hand, when increasing the electron density by a factor 10 to $n_0 = 2.0 \times 10^{14} \text{ m}^{-3}$, only the large damping lengths give high speed solar wind. The small damping lengths $H_m = 0.4 R_S$ and $L = 0.2 R_S$ give flow speeds at $r = 1 \text{ AU}$ of only $u_E = 170 \text{ km s}^{-1}$ and $u_E = 340 \text{ km s}^{-1}$, respectively, but still the large damping lengths, $H_m = 2.0 R_S$ and $L = 0.5 R_S$ give speeds as high as $u_E = 860 \text{ km s}^{-1}$ and $u_E = 950 \text{ km s}^{-1}$. The flow speeds above 1000 km s^{-1} are well above what is observed in the quasi-steady wind, and it can be argued that these results are not relevant for the solar wind. However, the model study serves to illustrate how sensitive the speed of the solar wind may be to the choices of the electron density in the inner corona.

In the rapidly expanding flow the expansion rate is larger than the electron–proton collision rate in the inner corona when the density is low. Then the thermal coupling between the electrons and protons is very weak, and almost all the energy flux deposited in the proton gas is lost in the solar wind. The solar wind proton flux is small, due to the low density at the inner boundary, and the asymptotic flow speed is large. The large flow speed is consistent with a large proton temperature in the corona. When the length scale, L , is decreased, a larger fraction of the energy flux is deposited in the subsonic region of the flow. Thus, the solar wind proton flux increases and the asymptotic flow speed decreases. When the coronal base electron density

is decreased, the solar wind proton flux is also decreased, and the asymptotic flow speed of the solar wind is increased. The results in Fig. 7 show that the coronal base electron density is very important for determining the fraction of the energy flux from the sun that is lost as kinetic and gravitational solar wind energy flux, in particular in rapidly expanding flow.

In spherically symmetric flow the expansion rate is reduced, and the electrons and protons are thermally coupled in the inner corona, also in the low density case, where $n_0 = 2.0 \times 10^{13} \text{ m}^{-3}$. This coupling leads to a larger solar wind proton flux, a smaller coronal proton temperature, and a lower asymptotic flow speed of the solar wind.

4. Conclusion

This model study shows that heating of the protons in the corona may lead to high proton temperature and large asymptotic flow speed of the solar wind. These solutions can be obtained when the electron density in the inner corona is low.

For spherically symmetric outflow the solar wind flow speed in the inner corona is low, and there is significant thermal coupling between electrons and protons, even for quite low electron densities. Thus, heating of the protons in the inner corona will lead to heat transfer to the electron gas and to a significant

heat conductive flux into the chromosphere–corona transition region. Most of this energy flux is lost as radiation from the transition region. The increase of the solar wind energy flux in the transition region is smaller than the radiative energy loss, so a significant inward heat flux is consistent with a quite large transition region pressure, a high electron density in the inner corona, a quite large solar wind proton flux, and a low asymptotic flow speed. By allowing for a more gradual damping of the energy flux from the sun, such that the outer corona is heated, we find a reduced proton flux and an increased asymptotic flow speed.

In rapidly expanding flow geometries the solar wind flow speed in the inner corona is higher than in spherically symmetric flow (for the same solar wind proton flux density at the orbit of Earth), the expansion rate of the plasma is larger, the thermal coupling between electrons and protons is weaker, and a smaller fraction of the energy flux deposited in the corona is lost as inward heat conductive flux. This may result in a more rapid acceleration and higher asymptotic speed of the solar wind than what we find in an $A \propto r^2$ flow geometry.

We conclude that in reasonable models of the corona–solar wind system, heating of the inner corona leads to a significant heat flux density into the transition region, a large transition region pressure, a large coronal base electron density, and a large solar wind proton flux. In order to obtain speeds comparable to the high speeds measured by the Ulysses spacecraft, a significant fraction of the energy flux from the sun must be deposited in the proton gas in the outer corona, where the proton heat conductive flux is small and the collisional coupling to the electrons is weak. This may lead to a low transition region pressure, a low coronal electron density, a high proton temperature, and a high asymptotic flow speed. Heating of the electron gas (as well as heating of the transition region and of the inner corona) will tend to increase the solar wind proton flux and reduce the asymptotic flow speed.

Acknowledgements. We thank Øystein Lie-Svendsen and Viggo H. Hansteen for comments on an earlier version of the manuscript. This work was supported by the Norwegian Research Council (NFR) under contracts 107781/432 and 115831/431 and by NASA grant W-18.786.

References

- Braginskii, S. I. 1965, in M. A. Leontovich (ed.), *Reviews of Plasma Physics*, Vol. 1, 205–311, Consultants Bureau, New York
- Feldman, W. C., Asbridge, J. R., Bame, S. J., Gosling, J. T. 1976, *J. Geophys. Res.*, 81, 5054
- Hammer, R. 1982a, *ApJ*, 259, 767
- Hammer, R. 1982b, *ApJ*, 259, 779
- Hansteen, V. H., Leer, E. 1995, *J. Geophys. Res.*, 100, 21577
- Hansteen, V. H., Leer, E., Holzer, T. E. 1997, *ApJ*, 482, 498
- Hollweg, J. V. 1973, *ApJ*, 181, 547
- Kohl, J. L., Strachan, L., Gardner, L. D. 1996, *ApJ*, 465, L141
- Landini, M., Monsignori-Fossi, B. C. 1973, *A&A*, 25, 9
- Leer, E., Holzer, T. E. 1980, *J. Geophys. Res.*, 85, 4681
- Leer, E., Holzer, T. E., Flå, T. 1982, *Space Sci. Rev.*, 33, 161
- Lie-Svendsen, O., Hansteen, V. H., Leer, E. 1997, *J. Geophys. Res.*, 102, 4 701
- McComas, D. J., Phillips, J. L., Bame, S. J. et al. 1995, *Space Sci. Rev.*, 72, 93
- McKenzie, J. F., Banaszkiewicz, M., Axford, W. I. 1995, *A&A*, 303, L45
- Olsen, E. L., Leer, E. 1996, *J. Geophys. Res.*, 101, 15591
- Parker, E. N. 1991, *ApJ*, 372, 719
- Phillips, J. L., Bame, S. J., Feldman, W. C. et al. 1995, *Sci*, 268, 1030
- Withbroe, G. L. 1988, *ApJ*, 325, 442